Astronomy & Astrophysics manuscript no. timingprecision7
December 8, 2016

TEE, a simple estimator for the precision of eclipse and transit minimum times

H. J. Deeg[1,2] and B. Tingley[3]

[1] Instituto de Astrofísica de Canarias, C. Via Lactea S/N, E-38205 La Laguna, Tenerife, Spain
[2] Universidad de La Laguna, Dept. de Astrofísica, E-38206 La Laguna, Tenerife, Spain
e-mail: hdeeg@iac.es
[3] Institut for Fysik og Astronomi, Aarhus Universitet, Ny Munkegade 120, 8000 Aarhus C, Denmark
e-mail: tingley@phys.au.dk

Received XXXX; accepted XXXX

ABSTRACT

Context. Transit or eclipse timing variations have proven to be a valuable tool in exoplanet research. However, no simple way to estimate the potential precision of such timing measures has been presented yet, nor are guidelines available regarding the relation between timing errors and sampling rate.
Aims. A 'timing error estimator' (TEE) equation is presented that requires only basic transit parameters as input. With the TEE, it is straightforward to estimate timing precisions both for actual data as well as for future instruments, such as the TESS and PLATO space missions.
Methods. A derivation of the timing error based on a trapezoidal transit shape is given. We also verify the TEE on realistically modeled transits using Monte Carlo simulations and determine its validity range, exploring in particular the interplay between ingress/egress times and sampling rates.
Results. The simulations show that the TEE gives timing errors very close to the correct one, as long as the temporal sampling is faster than transit ingress/egress durations and transits with very low S/N are avoided.
Conclusions. The TEE is a useful tool to estimate eclipse or transit timing errors in actual and future data-sets. In combination with an equation to estimate period errors (Deeg 2015), predictions for the ephemeris precision of long-coverage observations are possible as well. The tests for the TEE's validity-range led also to implications for instrumental design: Temporal sampling has to be faster than transit in- or egress durations, or a loss in timing-precision will occur. An application to the TESS mission shows that transits close to its detection limit will have timing uncertainties that exceed 1 hour within a few weeks after their acquisition. Prompt follow-up observations will be needed to avoid a 'loosing' of their ephemeris.

Key words. Methods: data analysis – Techniques:photometric – Ephemerides – Planets and satellites: detection – Occultations – binaries: eclipsing

1. Motivation for an estimator of eclipse and transit timing errors

The precise timing of stellar eclipses and planetary transits has a long track-record in astronomy, and numerous methods have been developed (e.g. Kwee & van Woerden 1956; Winkler 1967; Mikulášek et al. 2006; Oshagh et al. 2012) to measure the times of minimum brightness in eclipse-like events. Eclipse minimum times, translated into variations of orbital periods, have been widely used in the analysis of eclipsing binary systems. More recently they also became important in the analysis of light-curves from transiting exoplanets. In this case, deviations from strict periodicity, known as transit timing variations (TTV)', have usually been taken as a indication of the presence of additional bodies in the system (e.g. Agol et al. 2005; Holman & Murray 2005; Heyl & Gladman 2007). In such work, it is important to assure that a supposed TTV[1] is really due to an astrophysical effect and not an artefact of observational noise. This requires a technique to estimate of the precision of the measured transit ephemerides. This need for an estimation of timing and ephemeris errors also arose during the ground-based photometric follow-up of planet candidates from the CoRoT space mission (Deeg et al. 2009). In this case, a reliable estimator of the timing error was necessary to determine when and if follow-up photometric observations of a transit candidates should be scheduled – if the expected timing error exceeded a few hours, the observations would not be conclusive. During the course of the mission, we became aware that the errors in the ephemeris given to us – which had been derived by other members of the CoRoT-team – varied by factors of 'a few' for candidates with similar basic parameters, like brightness, transit-depth and transit-duration. Their ephemeris and their errors had been derived with a variety of methods, mostly by the fitting of different types of models, from trapezoid-shaped to more elaborate ones, but also 'eye-estimates' were used on occasion. A simple and reliable estimator to derive timing errors was therefore desirable in order to perform follow-up observations with little delay, which led to the method presented here. In combination with the estimator for period-errors presented in Deeg (2015), predictions for the time-uncertainty of future transits – which are essential for any follow-up observations – could now be performed quickly.

[1] In the remainder of this work, we use the terms 'transit' and 'eclipse' interchangeably

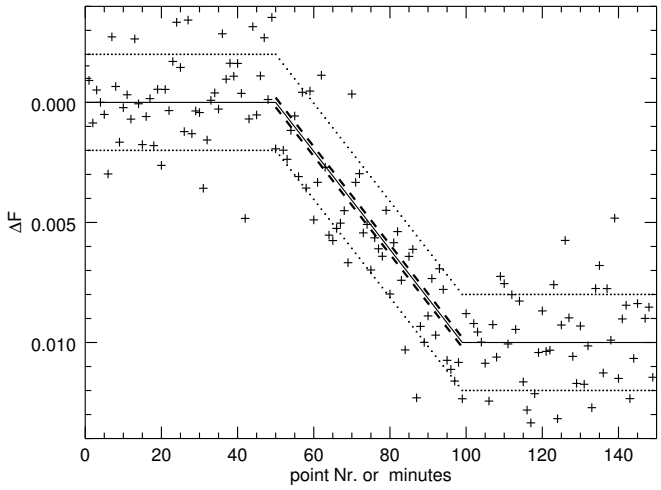

Fig. 1. Model of an eclipse ingress of $\Delta F = 0.01$ (solid line) with simulated data (crosses). The dotted lines outline the $\sigma_{F_{\rm rms}} = 0.002$ standard deviation of the individual data-points, and the dashed lines outline the expected error of the average over all 50 points within the ingress.

This work is distinct from other, similar works in the literature. The original work on the subject, which in part inspired this work, appeared in Doyle & Deeg (2004). Therein, the authors describe the timing error for triangular-shaped binary eclipses. This was later extended by Sybilski et al. (2010), who explored the detectability of TTVs in binary stars systems for the purpose of detecting circumbinary planets. They used a single eclipsing binary model and a single set of observing parameters (integration time, noise) for CoRoT and Kepler simulations and a few for ground-based simulations, ultimately verifying the equations presented in Doyle & Deeg (2004). Mighell & Plavchan (2013) and Deeg (2015) discuss ephemeris errors from continuous sets of timing measurements, covering multiple orbital periods, as given by data from space missions like CoRoT and Kepler. These latter papers however do not contemplate the expected timing precision of *individual* transit events, whose validation is the core of the present work.

Combining the work presented here and that by Deeg (2015) provides then the tools to derive both the epoch and the period-error of any linear ephemeris that is based on continous-coverage data, needing only basic eclipse or transit parameters. We expect this work to be of particular interest for the study of significance of transit timing variations (TTVs) as well as for the evaluation of timing precisions that can be expected in future instruments, such as the upcoming TESS and PLATO missions.

In the following, we present the formulae to derive timing errors of individual transits, which we refer to as the 'timing error estimator' (TEE). By using a trapezoidal approximation for the transit shape, it is possible to derive an analytical expression for the timing error of an individual transit based on a few basic parameters. We concentrate on the derivation of the timing error of individual eclipses and extend this by assessing the impact of sampling rate on the timing error. We begin by exploring trapezoidal model eclipses to verify that the expression works as expected, then extend it to real modelled exoplanetary transits.

2. The eclipse timing error estimator, TEE

The derivation of TEE arises from the use of a trapezoid to approximate the shape of the eclipse where the flat part being of any length, including zero. Furthermore, it assumes that the parameters of the trapezoid (amplitude and durations of ingress, flat part and egress) are known with negligible errors, such that the only free parameter is the time when the eclipse occurs. Under these conditions, the uncertainty in that time is identical to the error of the eclipse's central or minimum time. Given these assumptions, let us consider the ingress of an eclipse (Fig. 1), with a depth of 1% or $\Delta F = 0.01$. The observations are simulated by taking a model trapezoid and adding white noise, at a level of $\sigma_{F_{\rm rms}} = 0.002$ in the exemplified case. In real observations, the level of white noise would be derived from out-of-eclipse data. The white noise level during the ingress is then $\sigma_{F_{\rm in}} = \sigma_{F_{\rm rms}}/\sqrt{N_{\rm in}}$, where $N_{\rm in}$ is the number of points during ingress. In the event that the noise does not scale in this fashion, e.g. due to strong red noise, then $\sigma_{F_{\rm in}}$ should be determined by other means. The levels of $\pm\sigma_{F_{\rm in}}$ relative to the trapezoid are shown as dashed lines in Fig. 1. These lines also correspond to the expected 1σ errors when fitting the known model ingress to the data when the only free parameter is the time of ingress. The slope $T_{\rm in}/\Delta F$ determines then the corresponding error in time, given as $\sigma_{t_{\rm in}} = \sigma_{F_{\rm in}} T_{\rm in}/\Delta F$.

Considering that observations will generally contain both in-*and* egress, the only change is that instead of using only $\sigma_{F_{\rm Tin}}$, we should use the photometric noise on the time scale of ingress and egress summed, σ_{F_∇}, with T_∇ being the summed duration of ingress and egress (The ∇ symbol denotes ingress and egress, and is motivated by their triangular shape). This leads to the most basic form of the TEE[2]:

$$\sigma_{\rm t} = \frac{\sigma_{F_\nabla}\, T_\nabla}{2\,\Delta F} \tag{1}$$

were $\sigma_{\rm t}$ denotes the timing precision and $T_\nabla \approx 2T_{\rm in}$ was used.

We may also define a 'timing signal-to-noise', $(S/N)_t$, given by

$$(S/N)_t = 2\Delta F/\sigma_{F_\nabla}. \tag{2}$$

The relative timing error, $\sigma_{\rm t}/T_\nabla$, is then simply the inverse to $(S/N)_t$:

$$\frac{\sigma_{\rm t}}{T_\nabla} = \frac{1}{(S/N)_t} \tag{3}$$

Normally, the noise of the data on the time-scale T_∇ is not well known, but will be known on another time-scale τ (e.g. over the sampling time between data-points). We propose therefore a white-noise scaling from the known noise σ_{F_τ} over the time scale τ to that of $\sigma_{\rm F_\nabla}$ using

$$\sigma_{\rm F_\nabla} = \sigma_{F_\tau}\ \sqrt{\tau/T_\nabla} \tag{4}$$

were we assumed that the number of data points is proportional to the length of the time-scales τ and T_∇. This leads then to this general form of the TEE:

$$\sigma_{\rm t} = \frac{\sigma_{F_\tau}}{2\,\Delta F}\,\sqrt{\tau\, T_\nabla} \tag{5}$$

[2] While Eq. 1 uses relative values for the photometric noise σ_F and the transit amplitude ΔF, we note that for small amplitudes ΔF, the use of magnitude units for both parameters will lead to identical results

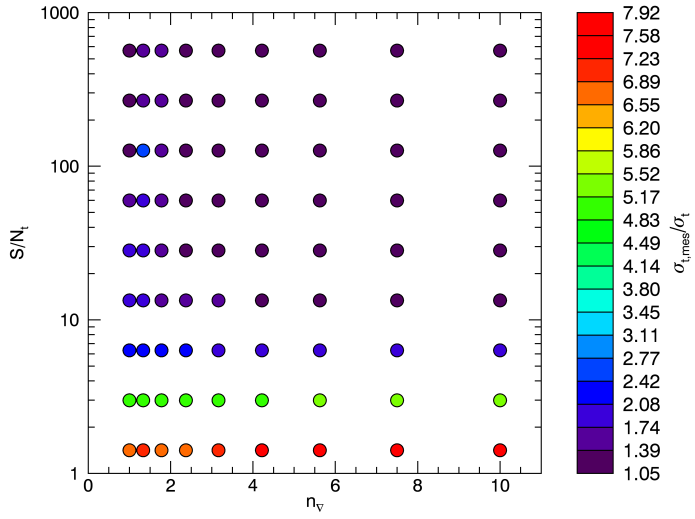

Fig. 2. Performance of the TEE based on simulations of trapezoid-shaped transits. The colour of each point indicates the ratio between the measured timing precision and the precision predicted by the TEE, $\sigma_{\rm t,meas}/\sigma_{\rm t}$, on the scale shown to the right. The measured precision has been derived from 10000 injection and retrieval simulations, for details see the text. The axes correspond to the simulations' input variables, which are the Signal-to-Noise relevant for timing precision (see Eq. 2) and n_∇, which is the combined number of points during ingress and egress.

For convenience, we also provide this equation in terms of the ingress time $T_{\rm in} = T_\nabla/2$:

$$\sigma_{\rm t} = \frac{\sigma_{F_\tau}}{\Delta F}\sqrt{\frac{\tau\, T_{\rm in}}{2}} \qquad (6)$$

In real time-series data, conversions between noises on different time-scales deviate often strongly from that for white noise when time-scales differing by more than an order of magnitude are considered. It is therefore advisable to characterise the noise on a time scale that is not very different from T_∇ when using TEE. For example, when we estimated of the timing precision for CoRoT transits, we measured the photometric noise over a timescale of τ=2 hours(Aigrain et al. 2009). This timescale is suitable as it is on the same order of magnitude as the T_∇ of the transit candidates. On the other hand, scaling from the point-to-point errors of CoRoT data would lead to an underestimation of the timing precision, as Aigrain et al. found a significant red noise contribution over a two-hour time scale relative to CoRoT's standard sampling time of 512 seconds. If, however, a white noise scaling from the point-to-point noise, $\sigma_{F_{\rm rms}}$, to σ_{F_∇} is acceptable, we may also use a version of the TEE in terms of the number of points during in-plus-egress, n_∇, with $n_\nabla = T_\nabla/\tau$ (with τ being here the time between exposures):

$$\sigma_{\rm t} = \frac{\sigma_{F_{\rm rms}}\, T_\nabla}{2\,\Delta F\,\sqrt{n_\nabla}} \qquad (7)$$

We note that above equation is well-suited for Kepler data, since no relevant red noise (Jenkins et al. 2010) affects the scaling from the nominal 30 minute sampling time of Kepler long cadence data to the hour-long in/egress durations of most planet transits, represented by T_∇ .

3. Scope and Limits to TEE

This theoretical equation requires a round of practical tests in order to demonstrate its validity. To this end, we perform two sets of Monte Carlo simulations based on model injection and parameter retrieval. First, we tested sets of modelled trapezoidal transits like those used to derive the TEE. Then, we did the same for sets of model transits like those we expect to encounter in nature. In both cases, we performed Monte Carlo simulations of these models to assess how well we could recover the transit timing, by fitting the known eclipse model to find the eclipse mid-times and then subtracting these from the input mid-times. This resulted in timing errors for each individual simulation. For each set of parameters, 'measured' timing errors $\sigma_{\rm t,meas}$ were then derived from the variance of timing errors from 10000 simulations. We then compared the measured errors to $\sigma_{\rm t}$, the timing errors expected from the TEE, via the ratio $\sigma_{\rm t,meas}/\sigma_{\rm t}$.

3.1. Behaviour of the TEE for trapezoidally shaped transits

The use of a trapezoidal shape in the first sets of simulations was motivated by the use of that same shape for the derivation the TEE, in order to determine the TEE's fundamental correctness and range of validity. The predicted relative timing error $\sigma_{\rm t}/T_\nabla$ depends only on one parameter, $(S/N)_t$ (see Eq. 2), but the range of $(S/N)_t$ for which the TEE is reliable was uncertain. Also uncertain was the range of validity of the TEE against another parameter that can be expected to affect the timing precision, the number of data points during in and egress, n_∇.

We used a Monte Carlo approach to obtain the $\sigma_{\rm t,meas}$. For each of the 10000 Monte Carlo trials, we generated 24-hour long time series with a specified sampling rate and level of white noise, and then inserted a trapezoidal event with a given value of n_∇ and $(S/N)_t$ at a random time $t_{\rm c}$ safely away from either end of the time series. Then, assuming *a priori* knowledge of the shape of the trapezoid, we endeavour to recover it with a simple χ^2 minimisation. We obtain a $\Delta t_{\rm c}$ from each trial by taking the difference with the input and output $t_{\rm c}$, keeping the χ^2 as an indication of the quality of the fit. The measured timing precision $\sigma_{\rm t,meas}$ is then obtained by taking the standard deviation of the values of $\Delta t_{\rm c}$ from the 10000 trails. This process is then repeated for each set of input parameters n_∇ and $(S/N)_t$.

The results from these simulations are shown in Fig. 2, expressed as the ratio between the measured timing precision and the one predicted by the TEE, $\sigma_{\rm t,meas}/\sigma_{\rm t}$. This ratio approaches 1, meaning that the TEE performs a valid prediction of the timing precisions, if two conditions are met: $n_\nabla > 2$ and $S/N_{\rm t} \gtrsim 10$. On the other hand, if the sampling rate or the S/N is below these limits, timing precisions may be much worse than given by the TEE.

Eq. 3 shows that for $S/N_{\rm t} \lesssim 1$, no useful timing error can be measured as $\sigma_{\rm t}$ will exceed the length of an in- or egress. In practice - and shown by the simulations - more stringent limits of $S/N_{\rm t}$ apply, since with decreasing S/N, the reliability of eclipse-detections decreases and contributions from random timing-results are increasing.

3.2. Behaviour of the TEE for naturally occurring transits

With the TEE against trapezoidally shaped transits being validated, we extend here the analysis to natural eclipse shapes, as these are of more practical interest. These tests are more complex than for the trapezoidal models that we used previously, as values such as T_∇ and ΔF are no longer input variables for

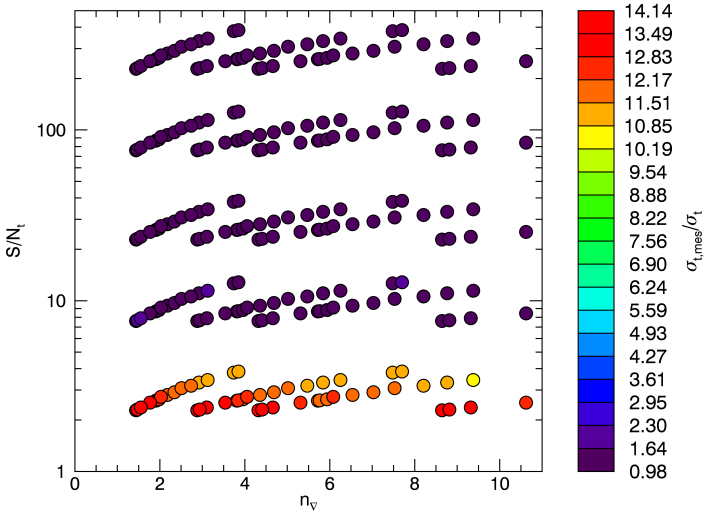

Fig. 3. Like Fig. 2 but from simulations using naturally shaped transits. The distribution of points does not adhere here to the grid apparent in Fig. 2, since the two parameters $((S/N)_t, n_\nabla)$ spanning this figure were calculated a posteriori from several input parameters that were varied between simulations (limb-darkening, impact parameter, sampling rate, white-noise level), see text.

the tests and must instead be approximated in some way in order to evaluate the accuracy of TEE. In theory, it should be possible to perform a numerical analysis of a model transit in order to calculate these values exactly. However, given the general uncertainties in transit parameters for the cases we expect to encounter, it is sufficient to the purposes of this study (which only attempts to evaluate the errors in timing, but not errors in other transit parameters) to fit trapezoids to naturally shaped transits, in order to derive the parameters that are relevant for the TEE. To that end, we proceeded in the following steps:

i) First, a set of noise-less model light-curves was generated from pixelated representations of a stellar disc that is occulted by a transiting planet, employing the same method as the UTM transit modeller (Deeg 2014). All models were generated for transits of a planet of 0.09 stellar radii across a solar-like star, while the following parameters were varied step-wise, leading to a total of 480 combinations: The impact parameter of the transit was incremented in 8 steps, from an equatorial transit with b=0 to a nearly-polar (but yet total) one with b=0.9. Models were generated with 6 different sampling rates, with the coarsest models representing the entire transit in 6 points and the finest ones representing it in 360 points. All models were generated for two visual passbands, namely V and I, using the corresponding quadratic solar limb-darkening coefficients. All of these models were then normalised such that the deepest part of the transit corresponds to a decrease in flux of $\Delta F = 1\%$. A further parameter, photometric white noise on 5 different levels, was added to the models only later, in step *iii*, but is already mentioned here: These noises had values ranging from $\sigma_{F_\tau} = 0.0001$ to 0.01, where the time-scale τ corresponds to a 1/6 of the total transit duration[3]. Each point in Fig. 3 corresponds to one of the possible parameter combinations[4].

ii) For each of these noise-less transit models, we obtained a trapezoidal fit and converted its output into the parameters relevant for the TEE, namely ΔF and T_∇ resp. n_∇. Since the models were those of real transits, the ΔF of the best-fit trapezoids was always lower than the 1% flux decrease of the input models. Also, due to the nature of the trapezoidal fit, the resulting fit duration was always longer than the transit duration of the input models.

iii) For each set of input parameters we performed 10 000 injection and retrieval trials. For each trial lightcurve, random white noise at one of the levels specified in step *i* was added to the noise-less models and the transit mid-time was offset by a random amount, which was recorded.

iv) On each of the trial lightcurves, we used the noise-less natural transit shape (obtained in step *i*) to perform a 1-parametric fit for the transit mid-time, and recorded the difference between the fitted mid-time and the input mid-time.

v) The subsequent analysis proceeded similarly to that of Sect. 3.1. That is, from the distribution of input-output differences from each of the 10 000 trials, we obtained the measured timing precision $\sigma_{\mathrm{t,meas}}$ and compared it to the TEE's estimate σ_t, which was based on the parameters from step *ii* and the known noise σ_{F_τ}. This was done for each parameter set, with the ratio $\sigma_{\mathrm{t,meas}}/\sigma_\mathrm{t}$ determining the colour of the points in Fig. 3.

We note that step *ii*'s use of a noise-less model to obtain the transit parameters except mid-time corresponds to the usual procedure employed in the analysis of long-coverage light-curves: There, transit parameters are derived from phase-wrapped superpositions of multiple individual transits, resulting in a light-curve with a higher S/N than that of the individual transits from which the timing measurements are being obtained.

The bulk of the sets in Fig. 3 shows a ratio $\sigma_{\mathrm{t,meas}}/\sigma_\mathrm{t}$ close to one, demonstrating that a trapezoidal fit to the transit is sufficient to estimate its expected timing error. However, a close comparison with the results from the trapezoidal tests depicted in Fig. 2 shows some subtle differences: reduced detectability for low values of $(S/N)_t \lesssim 3$, improved performance around $(S/N)_t \sim 7$, and in general a better performance for low values of n_∇. This is due to the fact that real transits have some curvature all the way through the transit. The T_∇ derived from the trapezoidal fit therefore underestimates the true effective value of this parameter, which mitigates the detrimental effects of low sampling rates. The differences for low $(S/N)_t$ may be real or may be an artefact of the fitting process. Either way, with the lowest S/N cases having timing errors σ_t that are larger than the transit duration, neither the transit-timings are reliably recovered nor are the transits themselves reliably detected.

4. An example application: Timing precision of TESS detections

In the following, we show an application of the TEE towards the estimation of the timing precision of transiting planets (or planet

[3] The indicated noises correspond therefore to the point-to-point noise in the models with the coarsest sampling. For models with finer sampling, the noises were incremented correspondingly, using a white-noise scaling.

[4] Only about half of the 480 possible parameter combinations are shown in Fig. 3, with the other half leading to values of n_∇ outside of the displayed range, up to $n_\nabla \approx 230$.

Table 1. Transit timing precision and ephemeris precision of example transit detections by the TESS mission. For explanation see text.

R_{pl} (R_{Earth})	R_* (R_{sun})	P_{pl} (day)	N_{tr}	I_c (mag)	σ_F (ppm/h$^{1/2}$)	ΔF (%)	$(S/N)_{det}$	T_∇ (sec)	N_∇	$\sigma_{F\nabla}$ (ppm)	$(S/N)_t$	σ_t (sec)	σ_P/P (x 10^{-4})	$\sigma_{T,1yr}$ (h)	sample *(ii - v*: relative to *i*)
2	1	9	3	11.6	474	0.0336	9.3	509	4.2	1261	0.5	956	8.7	6.95	*i*) near faint detection limit
2	0.3	9	3	14.8	4741	0.37	7.1	778	6.5	10199	0.7	1064	9.7	7.74	
4	1	9	3	13.6	1835	0.13	9.7	1018	8.5	3452	0.8	1309	11.9	9.52	
4	0.3	9	3	16.3	16752	1.49	8.3	1556	13	25479	1.2	1329	12.1	9.67	
2	1	9	3	9.1	136	0.03	32.4	509	4.2	362	1.9	274	2.5	2.00	
2	0.3	9	3	12.3	733	0.37	46.2	778	6.5	1577	4.7	165	1.5	1.20	*ii*) star 10x brighter
4	1	9	3	11.1	356	0.13	50.0	1018	8.5	669	4.0	254	2.3	1.84	
4	0.3	9	3	13.8	2138	1.49	65.1	1556	13	3252	9.2	170	1.5	1.23	
5	1	9	3	11.6	474	0.21	58.9	1272	11	797	5.3	242	2.2	1.76	
5	0.3	9	3	14.8	4741	2.33	46.5	1945	16	6450	7.2	269	2.4	1.96	*iii*) planet 2.5x larger
10	1	9	3	13.6	1835	0.84	62.2	2544	21	2183	7.7	331	3.0	2.41	
10	0.3	9	3	16.3	16752	9.32	56.0	3890	32	16115	11.6	336	3.1	2.45	
2	1	3	9	11.6	474	0.0336	13.4	353	2.9	1514	0.4	796	4.0	3.20	*iv*) $^1/_3$ orb. period, 3x more transits
2	0.3	3	9	14.8	4741	0.37	10.3	540	4.5	12248	0.6	886	4.4	3.57	
4	1	3	9	13.6	1835	0.13	14.0	706	5.9	4146	0.6	1090	5.4	4.39	
4	0.3	3	9	16.3	16752	1.49	12.0	1079	9	30599	1.0	1107	5.5	4.46	
5	1	9	3	9.1	136	0.21	205.1	1272	11	229	18.3	69	0.6	0.50	*v*) star 10x brighter and planet 2.5x larger
5	0.3	9	3	12.3	733	2.33	300.9	1945	16	997	46.7	42	0.4	0.30	
10	1	9	3	11.1	356	0.84	320.7	2544	21	423	39.7	64	0.6	0.47	
10	0.3	9	3	13.8	2138	9.32	439.1	3890	32	2056	90.7	43	0.4	0.31	

candidates) detected by the TESS mission. TESS (Ricker et al. 2014, 2015) is a NASA mission slanted for launch in late 2017 that will survey nearly the entire sky for transiting planets, with the majority of the sky being covered by single pointings lasting 27.4 days. This relatively short observational coverage may lead to concerns regarding the precision of the ephemeris of the transiting objects found, since ephemeris with large uncertainties may make the re-observation of a planet (or candidate - it does not matter in this context) very difficult. This becomes the case once a predicted transit has timing errors larger than 2-3 hours, which makes the appearance of that transit in a given observing night rather uncertain. During the photometric follow-up of CoRoT planet candidates (Deeg et al. 2009), this concern also surfaced, especially on candidates with shallow transits or on those found in 'short-run' pointings of less than 50 days. It led to the implementation of a timing-precision estimator for all candidates (Deeg et al. 2012) and motivated ongoing follow-up observations of all detected planets. These observations are being aimed at a refining of their ephemeris to a precision that maintains timing errors below 1 hour over at least one decade (Deeg et al. 2015). Table 4 shows **5** groups of examples with the timing precisions that can be expected from them by TESS. It also shows the corresponding precision of the ephemeris that may be obtained. The columns of that table are from left to right:

$R_{\rm pl}$, R_*: Sizes of the planet and the star.

$P_{\rm pl}$, $N_{\rm tr}$: Period of the planet and the number of transits that are observed by TESS, assuming its predominant temporal coverage of 27.4 days

I_C: Target magnitude in the I_C band of TESS. This band is at the centre of the TESS passband

σ_F: Expected 1-σ photometric precision for a target with given I_C magnitude over 1h integration time. This value was taken from the 'total precision' for a given magnitude in Fig. 8 of Ricker et al. (2015).

ΔF: Relative depth of a transit, assuming $\Delta F = (R_{\rm pl}/R_*)^2$, e.g. without limb-darkening.

$(S/N)_{\rm det}$: S/N of the transit detection. This value was obtained by scaling from the S/N = 7.3, quoted by Sullivan et al. (2015), for planet detections at the faint detection limit with a total on-transit duration of 6h.

T_∇: The duration of the combined in- and egress time for an equatorial transit. This value is derived for a circular orbit of the planet around its central star, with the planet-star distance derived from Kepler's third law, assuming a stellar mass given by the empirical mass-radius relation for main-sequence stars (Demircan & Kahraman 1991): $M_* = (R_*/1.06)^{(1/0.945)}$.

N_∇: Number of data-points in T_∇, the sum of ingress and egress time. The TESS time-sampling of 2 minutes is used.

σ_{F_∇}: Expected 1-σ photometric precision over the time-scale of T_∇.

$(S/N)_t$: 'Timing signal-to-noise', as defined by Eq. 2, for a single transit.

σ_t: Timing precision of single transits observed by TESS, derived from Eqs. 1 or 5, the latter one with $\tau = 1h$.

σ_P/P: Relative period-precision of the detected planet. σ_P was calculated from the formula by Deeg (2015) for the period error in a continuos set of timing measurements, given by $\sigma_P = \sigma_t\ (12/(N_{\rm tr}^3 - N_{\rm tr}))^{1/2}$.

$\sigma_{T,1\rm yr}$: Precision of the planet's ephemeris 1 year after the first transit was detected by TESS. For this value, Eq. 18 of Deeg (2015) was used, assuming σ_t to be the ephemeris' epoch (or zero-point) error. The dominant term of $\sigma_{T,1\rm yr}$ is however the period-error σ_P.

The first four cases (sample *i*) correspond to planet detections at the limiting I_C magnitude, from Fig. 3 of Sullivan et al. (2015), with a detection being defined by them as "achieving a signal-to-noise ratio greater than 7.3 from 6 hours of integration time during transits". Since it is impossible to generate planet-models with on-transit integration times of exactly 6 hours, the $(S/N)_{\rm det}$ of the four examples given deviates slightly from 7.3, with the actual S/N shown in the corresponding column. These four examples were selected to cover the range of stellar sizes that constitute the principal sample of TESS, and to cover the range of

planet-sizes for which Sullivan et al. calculated limiting magnitudes.

The next three samples *ii* - *iv* are identical to sample *i* except for the modification of a single parameter. In sample *ii*, the target stars are 10 times (or 2.5mag) brighter; in sample *iii* the planets' radii have been multiplied by 2.5, with the larger planets now about Jupiter-sized; and in sample *iv*, the orbital period has been divided by 3, leading to 3 times as many transit events. In sample *v*, both the planets' size and the target brightness have been increased relative to the cases at the detection limit.

Regarding the interpretation of these calculations, first we note that in all cases, the derived timing precisions are *lower* limits to the timing precisions due to assuming equatorial transits where in/egress times are shortest, and due to neglecting stellar limb-darkening, which also leads to in/egress times that may be shorter – but never longer – than the transit in/egresses in real cases, where the inner part often displays a notable rounding as well. Even with these shortest-possible in/egress times, we find that N_{∇} is $\gtrsim 3$ in all cases, meaning that TESS' 2-minute sampling-interval is sufficiently short to avoid any degradation of the timing-precision.

For the cases at the faint detection limit (sample *i*), their theoretical timing error σ_t is about 15-20 minutes, while the error of the ephemeris of such planets (or planet-candidates) will be on the order of an hour within 1 - 2 months, and their re-observation after one year will be be rather difficult, with timing uncertainties that may be as large as ± 10 hours. A further warning on the observability of these detections is due to their very low timing Signal-to-noise $(S/N)_t$, which is around unity. As our simulations in Sect. 3 have shown, true timing errors will exceed the theoretical errors for $(S/N)_t \lesssim 10$, while timing measures may become impossible for $(S/N)_t \lesssim 1$, with timing-errors σ_t that are similar or exceed the duration of in and egress (T_{∇}). Such very low values of $(S/N)_t$ may also cast doubts on the overall detectability of the transits of these limiting cases. This is however an issue that we consider outside of the scope of this work, referring here to the simulations of Sullivan et al. (2015).

For samples *ii* and *iii*, with a detection S/N of about 50, we expect that one year after the observations by TESS, the ephemeris-errors will be about 2 hours. That is, there is a maximum of about one year to perform follow-up up observations before multi-night or multi-site campaigns may become required to 'recover' the transits of a given planet. Sample *iv* evaluates the gain from shorter orbital periods. The timing precision of individual transits (σ_t in Table 4) improves only slightly over sample *i*, due to the shorter in and egress-times (T_{∇}). The larger number of observed transits leads however to an improvement in the ephemeris precision (σ_P/P and $\sigma_{T,1\mathrm{yr}}$) by a factor of ≈2. For such planets, with a detection S/N of 10-15, follow-up observations would be needed within a few months.

Only for sample *v*, with a detection S/N higher than 200, will TESS derive ephemeris that are sufficiently precise to permit re-observation of their transits for several years. A refinement of these ephemeris by a dedicated follow-up program would however be desirable as well, in order to obtain ephemeris that are sufficiently precise for useful transit-predictions over time-scales of 10 years or more.

5. Conclusions

In this work we have introduced and validated the TEE, a formula that permits a quick estimation of the expected timing precisions of individual transits or eclipses. This is expected to be useful for estimates of timing-precisions for both ground and space-based data. Together with the work by Deeg (2015) about period and ephemeris errors from time-series covering multiple orbital periods, and assuming that there are no intrinsic period variations (e.g. Transit timing variations, TTVs), we now have the tools at hand to estimate the ephemeris precision for the majority of planet detections (those without TTVs) from rather basic assumptions, as is shown in the preceding example on TESS detections.

From the simulations shown in Sect. 3, we can conclude that the TEE accurately represents the timing precision of idealised trapezoidal eclipses, provided that the timing signal-to-noise is $(S/N)_t > 10$ and the number data-points during in and egress, n_{∇}, is larger than 2. While Eq. 3 shows that no useful timing error can be measured for $(S/N)_t \lesssim 1$, as σ_t will exceed the length of an in- or egress, in practice more stringent limits of $(S/N)_t$ may apply, since eclipses with low $(S/N)_t$ will also have a low reliability to be detected at all. The TEE also predicts the timing error of naturally occurring transits, for which it is sufficient to obtain the TEE's required parameters from trapezoidal fits to the transits. Moreover, the limitations on timing precision from low n_{∇} seem to have a lesser effect on natural transits, as they have, in general, no truly flat portions – it is not the flat portion of a trapezoidal eclipse that contributes to the timing precision, but the slopes of the ingress/egress. We note that one of the assumptions in the TEE are negligible errors in its input parameters (f.ex. the depth of the transit). Considering that the TEE estimates not a value but an error - for which 1-2 digit precision is sufficient - this assumption should not have consequences in practical applications. In any case, relevant uncertainties of the input parameters will occur only in the low S/N regime, were our simulations have already shown that the results from the TEE lead to underestimations of the real timing-error. We emphasize here that the TEE is not intended to generate 'final' publication-quality timing-errors if a full transit-modeling is feasible.

The results from our simulations also have implications for the observational design of instruments acquiring photometric time series. As a general rule, eclipses or transits should be observed with cadences that are shorter than the expected in- or egress duration (e.g. $n_{\mathrm{in}} > 1$ is desirable). Beyond this, and assuming that a white-noise scaling is valid, the number of data-points during in or egress has little effect neither on the real timing precision nor on the reliability of prediction made with the TEE.

As an example of this, the Kepler/K2 mission obtained most of its target time-series with its 'long cadence' (29.4 min) sampling. For eclipsing bodies that are small or short periodic, in/egress times shorter than 30 min are frequently encountered. The timing precisions of these short periodic objects would have been substantially better if they would have been observed with cycle times a half or a quarter as long than the long cadence. For example, Ford et al. (2011)indicate an improvement in the timing error of the KOI-137 system (published in parallel as Kepler 18 by Cochran et al. 2011) of a factor of two for its short-cadence (≈ 1 min sampling) data relative to its long cadence data.

Regarding the TESS mission, our calculations on expected ephemeris precisions have shown that a rapid photometric follow-up to acquire further eclipse times will be essential to maintain future observability of transiting planets found near the TESS detection limit. Also, for the majority of its expected planet discoveries, further photometric follow-up will be required in order to establish ephemeris that guarantee their long-term observability.

This will not be a worry with the PLATO space mission, foreseen to be launched by ESO in late 2025, which will ob-

serve large swaths of the sky with campaigns lasting 2-3 years (Rauer et al. 2014). PLATO's nominal sampling rate of 25 seconds (with bright objects being sampled with a rate of 2.5 seconds) largely exceeds the sampling requirements for precision timing of any kind of normal planet-star system. It may have other benefits, however, such as a more reliable recovery of the shapes of eclipses from short-periodic orbiters or the timing of eclipses across compact objects, such as white dwarfs, where total eclipse durations on the order of minutes may be encountered.

Acknowledgements. We thank the anonymous referee for comments that led to a significant improvement in the presentation of this work. HD acknowledges support by grants AYA2012-39346-C02-02 and ESP2015-65712-C5-4-R, both of the Spanish Secretary of State for R&D&i (MINECO).

References

Agol, E., Steffen, J., Sari, R., & Clarkson, W. 2005, MNRAS, 359, 567
Aigrain, S., Pont, F., Fressin, F., et al. 2009, A&A, 506, 425
Cochran, W. D., Fabrycky, D. C., Torres, G., et al. 2011, ApJS, 197, 7
Deeg, H. J. 2014, UTM: Universal Transit Modeller, Astrophysics Source Code Library
Deeg, H. J. 2015, A&A, 578, A17
Deeg, H. J., Gillon, M., Shporer, A., et al. 2009, A&A, 506, 343
Deeg, H. J., Klagyivik, P., Alonso, R., & Hoyer, S. 2015, in European Physical Journal Web of Conferences, Vol. 101, European Physical Journal Web of Conferences, 06020
Deeg, H. J., Seidel, M., & the Corot Photometric Follow-Up Team. 2012, ArXiv e-prints
Demircan, O. & Kahraman, G. 1991, Ap&SS, 181, 313
Doyle, L. R. & Deeg, H.-J. 2004, in IAU Symposium, Vol. 213, Bioastronomy 2002: Life Among the Stars, ed. R. Norris & F. Stootman, 80
Ford, E. B., Rowe, J. F., Fabrycky, D. C., et al. 2011, ApJS, 197, 2
Heyl, J. S. & Gladman, B. J. 2007, MNRAS, 377, 1511
Holman, M. J. & Murray, N. W. 2005, Science, 307, 1288
Jenkins, J. M., Caldwell, D. A., Chandrasekaran, H., et al. 2010, ApJ, 713, L120
Kwee, K. K. & van Woerden, H. 1956, Bull. Astron. Inst. Netherlands, 12, 327
Mighell, K. J. & Plavchan, P. 2013, AJ, 145, 148
Mikulášek, Z., Wolf, M., Zejda, M., & Pecharová, P. 2006, Ap&SS, 304, 363
Oshagh, M., Boué, G., Haghighipour, N., et al. 2012, A&A, 540, A62
Rauer, H., Catala, C., Aerts, C., et al. 2014, Experimental Astronomy, 38, 249
Ricker, G. R., Winn, J. N., Vanderspek, R., et al. 2014, in Proc. SPIE, Vol. 9143, Space Telescopes and Instrumentation 2014: Optical, Infrared, and Millimeter Wave, 914320
Ricker, G. R., Winn, J. N., Vanderspek, R., et al. 2015, Journal of Astronomical Telescopes, Instruments, and Systems, 1, 014003
Sullivan, P. W., Winn, J. N., Berta-Thompson, Z. K., et al. 2015, ApJ, 809, 77
Sybilski, P., Konacki, M., & Kozłowski, S. 2010, MNRAS, 405, 657
Winkler, L. 1967, AJ, 72, 226